Polymer Bulletin (2023) 80:6433–6454
https://doi.org/10.1007/s00289-022-04363-3

ORIGINAL PAPER

Synthesis, characterization, and biological activities of new conjugates of Guanosine grafted on polyvinyl alcohol, carbohydrate chitosan, and cellulose

Sabry A. El-Naggar[1] · Ahmed A. El-Barbary[2] · Yehia A. Hafez[2] · Wesam M. Salama[1] · Hazem M. Elkholy[2] · Mohamed Shaker[2]

Received: 22 January 2022 / Revised: 23 June 2022 / Accepted: 25 June 2022 /
Published online: 18 July 2022
© The Author(s) 2022

Abstract

Guanosine (GU) is a purine nucleoside that has different biological applications. This study aimed to synthesize, characterize, and enhance the biological activities of GU through its covalently grafting on polyvinyl alcohol (PVA), chitosan (CS), and cellulose (CL). In this regard, the conjugation was constructed by different linkers such as chloroacetyl chloride, 2-bromopropionyl bromide, and epichlorohydrin (EPCH). The resulted novel conjugates were characterized by FT-IR, ^{1}H-NMR, GPC, and TGA techniques. FT-IR spectra revealed the main characteristic groups, O–H, N–H, C=O and C=N of GU moieties. Furthermore, ^{1}H-NMR spectra showed the aromatic C–H, O–H, and N–H protons of the grafted GU moieties. Two decomposition stages of grated polymers with high thermal stability are illustrated by TGA. GU showed no antifungal activity against *Aspergillus fumigatus* and *Candida albicans*. However, its conjugates: P-1A, P-1B, P-2A, P-2B, P-3A, and P-3B displayed significant antifungal effect with inhibitory zones in the range 8–11 mm. As compared to GU group, most of GU-polymer conjugates showed significant in vivo antitumor activity against EAC-bearing mice via the reduction in total tumor volume. In summary, these conjugates are biologically active macromolecules and may act as candidate carrier systems for other applications such as drug delivery.

Keywords Polyvinyl alcohol · Chitosan · Cellulose · Guanosine · Antifungal · Antitumor

✉ Hazem M. Elkholy
Hazem_elkholy@science.tanta.edu.eg; dr.hazem3010@gmail.com

[1] Zoology Department, Faculty of Science, Tanta University, Tanta 31527, Egypt

[2] Chemistry Department, Faculty of Science, Tanta University, Tanta 31527, Egypt

Introduction

Biocompatible polyvinyl alcohol (PVA) has high mechanical resistance, chemical stability, large surface area, and low toxicity, which gives it a high variety in clinical applications [1]. Previous studies reported that PVA was functionalized with chloroacetate groups by treatment with chloroacetyl chloride followed by coupling with sodium salt of salicylic acid for controlled drug release [2]. In another study, the crosslinking of PVA with xanthan using EPCH under basic conditions showed important drug release properties [3]. PVA phosphorylation was performed through its oxidation to form vinyl ketone and reaction with phosphorylating agents [4]. Carboxymethyl cellulose and PVA were cross-linked with EPCH to form polymer-drug systems for sustained release of chloramphenicol [5]. Furthermore, PVA and chitosan (CS) were chemically cross-linked with EPCH to yield hybrid hydrogels for potential use in tissue engineering [6].

CS is a natural linear polysaccharide consisting of randomly dispersed β-(1–4-D-glucosamine and *N*-acetyl-D-glucosamine [7]. The free amino and hydroxyl groups of CS cause its solubility in acidic solutions for chemical functionalization [8]. CS possesses diverse activities such as biocompatibility, biodegradability, non-toxicity, anti-inflammatory, antihypertensive, and antimicrobial behavior [9–11]. In addition, it showed great potential applications in drug delivery systems, agriculture, textiles, food, medical, and cosmetic industries [12–15]. The crosslinking of CS was performed through its hydroxyl groups with EPCH after protection of amino groups with benzaldehyde to form the corresponding Schiff base polymers for metal removal and dye adsorption applications [16–20]. Acyl thiourea/CS conjugates were obtained by treatment of CS with acyl thiocyanate. These conjugates displayed antimicrobial activities in vitro [21]. Polypeptide/CS conjugate was formed through ring-opening copolymerization of CS with some amino acids, *N*-carboxy anhydrides, lactones, oxiranes as well as 2-alkyl oxazolines [22]. CS-spiroquinazolinone conjugates were prepared via coupling of CS with benzoxazinyl benzoic acid, and these conjugates provided significant antimicrobial activity [23]. The grafting of CS with different 1,3,4-oxadiazoles provided biologically active conjugates that have insecticidal activity against cotton leafworm *Spodoptera littoralis* [24].

Cellulose (CL) is a polysaccharide consisting of a linear chain of several β(1 → 4) linked D-glucose units [25] and is a main component of the primary cell wall of green plants [26]. The cross-connection of CL with EPCH formed polymeric adsorbents [27]. In the structural modification, CL chloroacetate was grafted with styrene, methyl methacrylate, acrylomorpholine and/or methacrylamide by atom-transfer radical polymerization [28, 29]. Moreover, chloroacetate CL ester was prepared and grafted with monopyridyl tritolylporphyrin [30]. The synthetic strategy for the preparation of starch derivatives bearing aminopyridinium groups (2-aminopyridine, 3-aminopyridine, 4-aminopyridine, 2,3-diaminopyridine, 2,6-diaminopyridine, and 3,4-diaminopyridine) was performed through starch functionalization with chloroacetyl chloride molecule [31]. CL-based magnetic nano-composite functionalized with -SO_3H groups was synthesized to promote the synthesis of pyrimido [4,5-b] quinolone and pyrido [2,3-d] pyrimidine derivatives [32].

GU is a purine nucleoside thought to possess neuroprotective properties [33]. A study of the anticancer effect of an oxidized form of thioguanosine (sulfinosine) showed an induction of caspase-dependent apoptotic cell death and autophagy in glioma cells. Furthermore, sulfinosine increases reactive oxygen species and decreases the antioxidant peptide glutathione levels [34]. In cancer studies, GU induces melanoma cell differentiation in the protein kinase C/ extracellular signal-regulated kinase pathway, increasing dendritogenesis, melanogenesis, and decreasing cell motility [35]. GU and temozolomide cause cytotoxicity in human A172 glioma cells. A change in mitochondrial membrane potential and an increase in apoptosis are resulted from the combination of these compounds [36]. GU-inferred supramolecular hydrogels have guarantee in the fields of medication conveyance, directed discharge, and tissue design applications [37]. Isoguanosine gel illustrated anticancer activities for a variety of cancer cells with dual-functions such as delivery system and anticancer compound in one system [38]. The chemical grafting of modified PVA, CS, and CL with folic acid by different linkers showed enhancing in the biological applications of folic acid [39]. The novelty of this study was conducted to synthesize, characterize and enhance the biological activities of PVA, CS, and CL via grafting with GU by using different linkers such as chloroacetyl chloride, 2-bromopropionyl bromide, and EPCH. *Aspergillus fumigatus* and *Candida albicans* were selected as fungal strains to study and compare the antifungal effect of GU and its polymer conjugates. GU showed no antifungal activity, while after its chemical conjugation with the modified polymers, the antifungal activity improved. In addition, EAC-bearing mice model was used to assess and compare the antitumor activity of GU and its polymer conjugates.

Materials and methods

Chemicals

Polyvinyl alcohol (PVA) (Degree of hydrolysis, 98%), chitosan (CS) (82% degree of deacetylation determined by titration [24], molecular weight 100,000–300,000 g/mol), microcrystalline cellulose (CL), chloroacetyl chloride, 2-bromopropionyl bromide, triethylamine (TEA), guanosine (GU), *N*-methyl-2-pyrrolidone (NMP), epichlorohydrin (EPCH), ketoconazole and cisplatin (CIS) were purchased from Sigma-Aldrich, Germany (Distributor, Egyptian International Center For Import, Naser City, Egypt).

Synthesis of GU polymer conjugates

Synthesis of poly(vinyl chloroacetate) (PVCA) and poly(vinyl bromopropionate) (PVBP)

Polyvinyl alcohol (4 g) was dissolved in dimethylformamide (DMF) (60 mL) by heating, and chloroacetylchloride and/or 2-bromopropionyl bromide (20 mL)

were added. The reaction mixture was refluxed for 1 h, cooled, and poured over a large amount of water. The products were filtered off, washed several times with water, and dried at 50 °C for one week [39, 40].

PVCA: FT-IR (film on KBr plate) (Fig. 1): v (cm^{-1}) 2790 (aliph. C-H), 1736 (st. C = O), 1468 (st. C–C), 1213 (st. C-O), 641 (st. C–Cl).

PVBP: FT-IR (film on KBr plate) (Fig. 1): *v* (cm^{-1}) 2788 (aliph. C-H), 1723 (st. C = O), 1467 (st. C–C), 1238 (st. C-O), 507 (st. C–Br).

Synthesis of chitosan chloroacetate (CSCA) and chitosan bromopropionate (CSBP)

A mixture of carbohydrate CS (3 g) and chloroacetylchloride and/or 2-bromopropionyl bromide (30 mL) was refluxed in NMP (40 mL) for 1 h. The reaction mixture was cooled and poured over a large amount of water. The products were filtered off, washed several times with water, and dried at 50 oC for one week [31, 41].

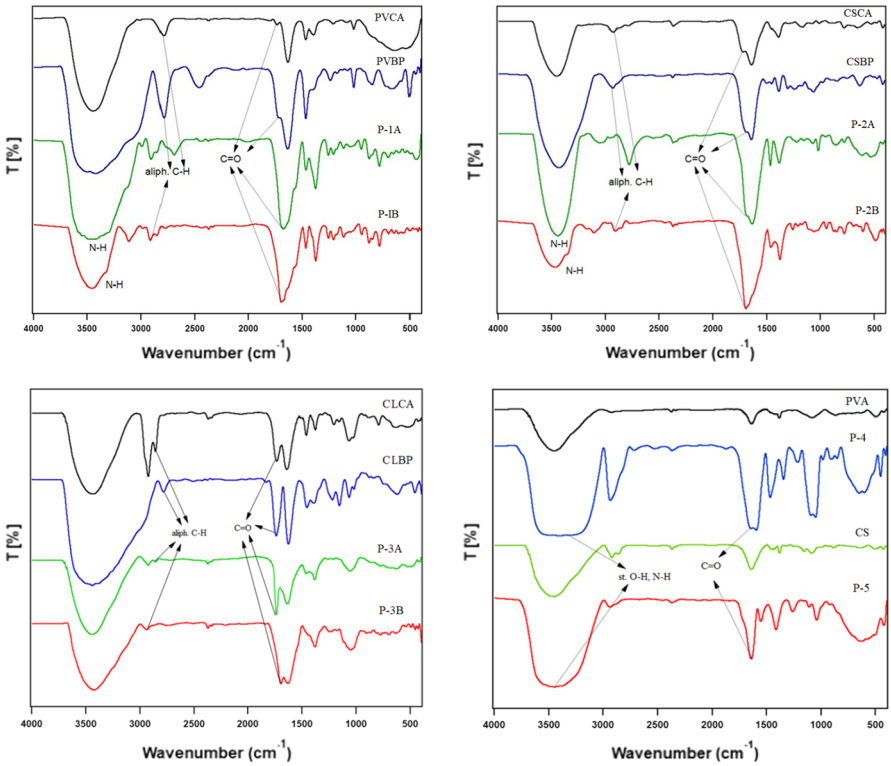

Fig. 1 FT-IR spectra of PVCA, PVBP, P-1A, P-1B, CSCA, CSBP, P-2A, P-2B, CLCA, CLBP, P-3A, P-3B, PVA, P-4, CS and P-5

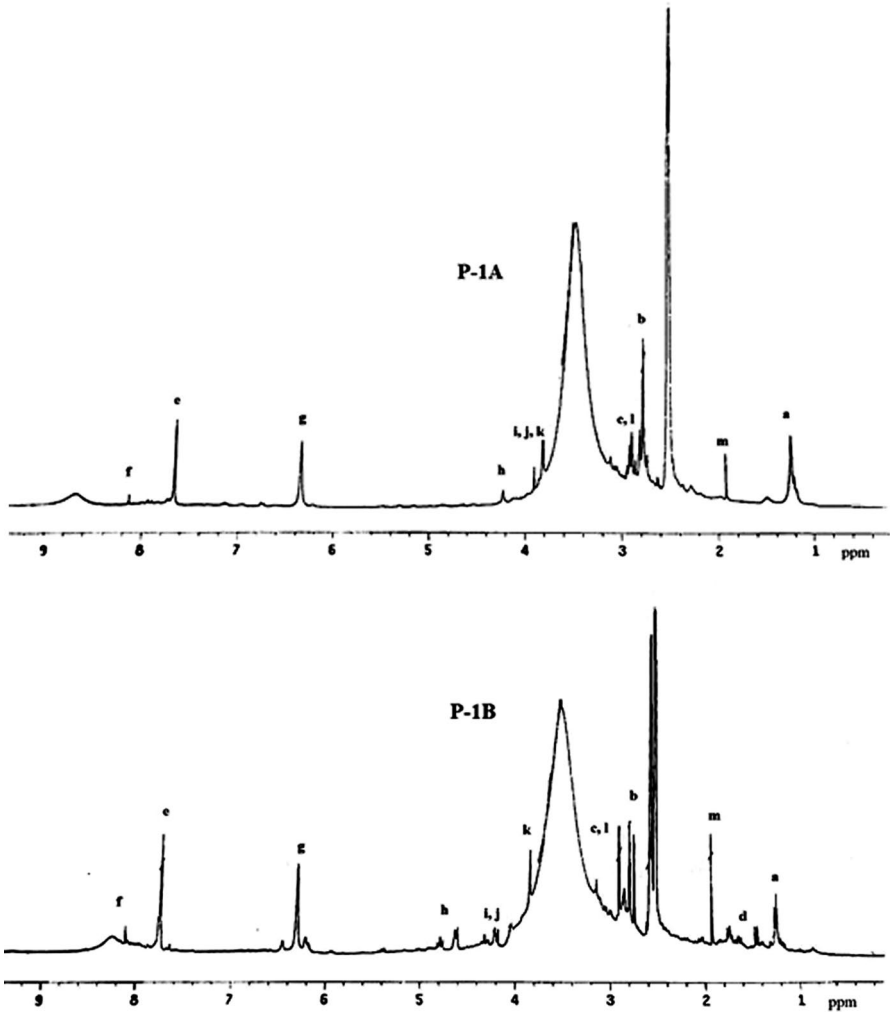

Fig. 2 ^{1}H-NMR spectra of polymers P-1A and P-1B

CSCA: FT-IR (film on KBr plate) (Fig. 2): v (cm^{-1}) 3455 (st. NH), 2927 (aliph. C-H), 1737 (st. C = O), 1391 (st. C–C), 1169 (st. C-O), 781 (st. C–Cl).

CSBP: FT-IR (film on KBr plate) (Fig. 2): *v* (cm^{-1}) 3430 (st. NH), 2931 (aliph. C-H), 1705 (st. C = O), 1387 (st. C–C), 1243 (st. C-O), 634 (st. C–Br).

Synthesis of cellulose chloroacetate (CLCA) and cellulose bromopropionate (CLBP)

Carbohydrate CL (2.5 g) was suspended in DMF (30 mL) by heating, and chloroacetylchloride and/or 2-bromopropionyl bromide (10 mL) were added. The reaction mixture was refluxed for 1 h, cooled, and poured over large amounts of water. The

products were filtered off, washed several times with water, and dried at 50 oC for one week [30, 39].

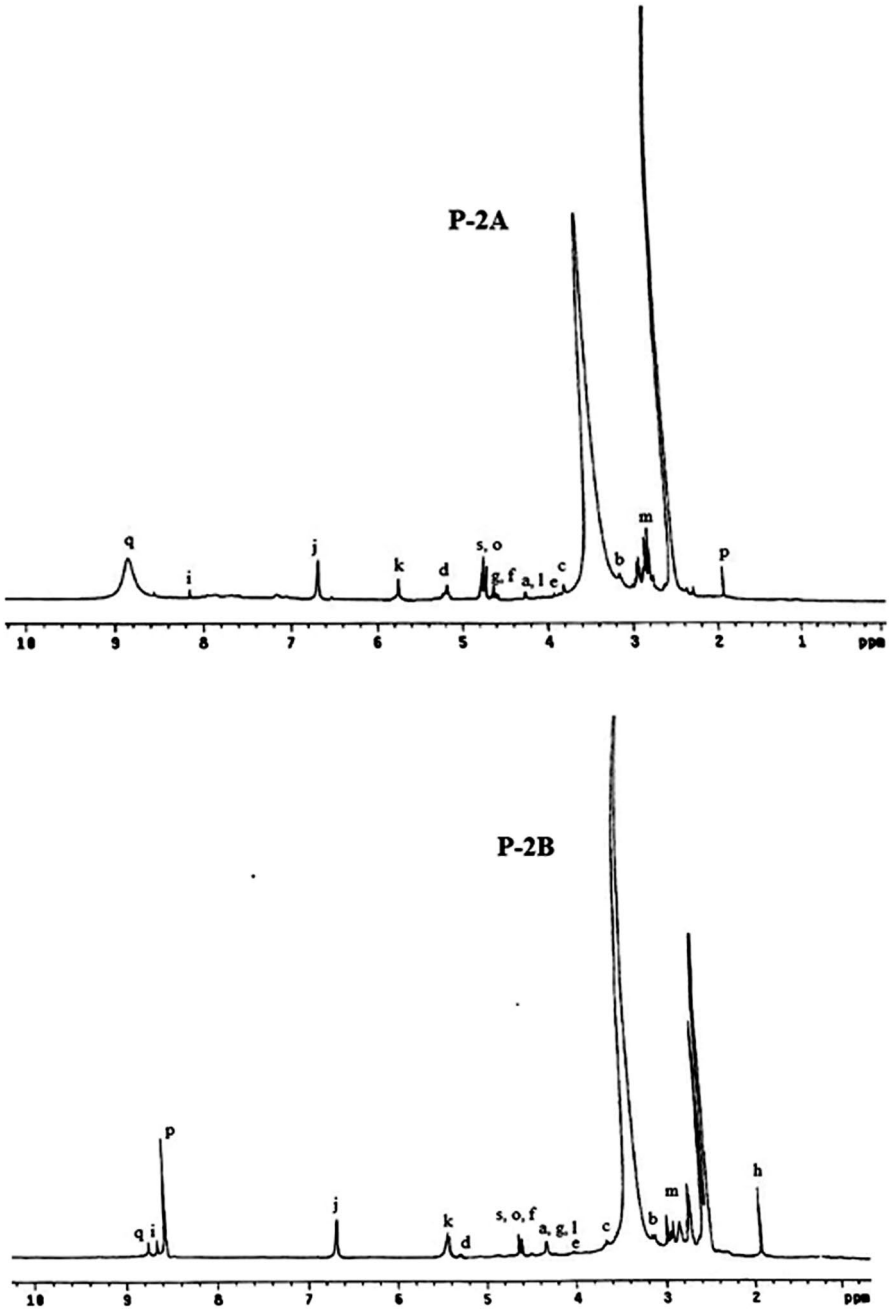

Fig. 3 ^{1}H-NMR spectra of polymers P-2A and P-2B

CLCA: FT-IR (film on KBr plate) (Fig. 3): ν (cm^{-1}) 3450 (st. OH), 2920, 2860 (aliph. C-H), 1740 (st. C = O), 1465 (st. C–C), 1210 (st. C-O), 797 (st. C–Cl).

CLBP: FT-IR (film on KBr plate) (Fig. 3): ν (cm^{-1}) 3438 (st. OH), 2783 (aliph. C-H), 1741 (st. C = O), 1386 (st. C–C), 1220 (st. C-O), 624 (st. C–Br).

Synthesis of poly(vinyl chloroacetate)-grafted-GU (P-1A) and poly(vinyl bromopropionate)-grafted-GU (P-1B)

A mixture of PVCA and/or PVBP (1 g), TEA (1 mL) and GU (8.2 and/or 5.6 mmoL) was dissolved in DMF (30 mL). The reaction mixture was warmed at 100 °C for 3 days (tlc), and the solvent was removed under vacuum. The products were collected, washed several times with acetone, and dried at 50 °C for 2 days [39].

Polymer P-1A: FT-IR (film on KBr plate) (Fig. 1): ν (cm^{-1}) 3450 (st. OH), 3397 (st, NH), 3120 (st, H-C = C), 2992, 2907, 2696 (aliph. C-H), 1690 (st. C = O), 1565 (st, C = C), 1467 (st. C = N), 1377 (st. C–C), 1211 (st. C-O), 781 (st. C–Cl). ^{1}H-NMR (DMSO-d_6) (Fig. 2): δ (ppm) = 1.18–1.23 (*m*, CH_2 (protons a)), 1.91 (*s*, OH (protons m)), 2.71–2.81 (*m*, CH (protons b)), 2.89–2.94 (*m*, CH, CH_2 (protons c, l)), 3.82–3.94 (*m*, CH (protons i, j, k)), 4.22 (*m*, CH (protons h)), 6.35 (*s*, ar. CH (protons g)), 7.67, 8.16 (*s*, NH (protons e, f)).

Polymer P-1B: FT-IR (film on KBr plate) (Fig. 1): ν (cm^{-1}) 3458 (st. OH), 3330 (st, NH), 3112 (st, H-C = C), 2985, 2913, 2852 (aliph. C-H), 1697, 1683 (st. C = O), 1570 (st, C = C), 1468 (st. C = N), 1375 (st. C–C), 1209 (st. C-O), 515 (st. C–Br). ^{1}H-NMR (DMSO-d_6) (Fig. 2): δ (ppm) = 1.22–1.29 (*m*, CH_2 (protons a)), 1.42–1.74 (*m*, CH_3 (protons d)), 1.91 (*s*, OH (protons m)), 2.73–2.78 (*m*, CH (protons b)), 2.83–2.89 (*m*, CH, CH_2 (protons c, l)), 3.83–4.31 (*m*, CH (protons i, j, k)), 4.61–4.79 (*m*, CH (protons h)), 6.32 (*s*, ar. CH (protons g)), 7.77, 8.15 (*s*, NH (protons e, f)).

Synthesis of chitosan chloroacetate-grafted-GU (P-2A) and chitosan bromopropionate-grafted-GU (P-2B)

A mixture of CSCA and/or CSBP (1 g), TEA (0.3 mL) and GU (2.65 mmoL) was dissolved in DMF (30 mL). The reaction mixture was warmed at 100 °C for 3 days (tlc), and the solvent was removed under vacuum. The products were collected, washed several times with acetone, and dried at 50 °C for 2 days [39].

Polymer P-2A: FT-IR (film on KBr plate) (Fig. 1): ν (cm^{-1}) 3442 (st. OH) 3060 (st. NH), 3020 (st, H-C = C), 2953, 2780 (aliph. C-H), 1692 (st. C = O), 1468 (st, C = C), 1347 (st. C = N), 1222 (st. C–C), 1157 (st. C–O), 779 (st. C–Cl). ^{1}H-NMR (DMSO-d_6) (Fig. 3): δ (ppm) = 1.86 (*s*, OH), 2.76–2.89 (*m*, CH_2 (protons m)), 3.16 (*m*, CH (protons b)), 3.81 (*m*, CH (protons c)), 3.92 (*m,* CH (protons e)), 4.28 (*m*, CH, CH_2 (protons a, l)), 4.58–4.64 (*m*, CH_2, CH (protons g, d)), 4.71–4.83 (*m*, CH (protons s, o)), 5.19 (*m*, CH (protons f)), 5.71, (*d*, CH (protons k)), 6.71 (CH (protons j)), 8.19, 8.84 (*s*, NH (protons i, q)).

Polymer P-2B: FT-IR (film on KBr plate) (Fig. 1): *v* (cm^{-1}) 3476 (st. OH), 3181 (st, NH), 3108 (st, H-C = C), 2976, 2909 (aliph. C-H), 1695 (st. C = O), 1467 (st, C = C), 1377 (st. C = N), 1257 (st. C–C), 1211 (st. C-O), 494 (st. C–Br). ^{1}H-NMR (DMSO-d_6) (Fig. 3): δ (ppm) = 1.96 (*d*, CH_3 (protons h)), 2.76–2.89 (*m*, CH_2 (protons m)), 3.09–3.12 (*m*, CH (protons b)), 3.62 (*m*, CH (protons c)), 4.03 (*m,* CH (protons e)), 4.33 (*m*, CH_2, CH, CH (protons a, g, l)), 4.58–4.62 (*m*, CH (protons s, o, d)), 5.31 (*m*, CH (protons f)), 5.44, (*d*, CH (protons k)), 6.69 (*s,* CH (protons j)), 8.56, (*s*, OH (protons p)), 8.65, 8.78 (*s*, NH (protons i, q)).

Synthesis of cellulose chloroacetate-grafted-GU (P-3A) and cellulose bromopropionate-grafted-GU (P-3B)

A mixture of CLCA and/or CLBP (0.7 g), TEA (0.3 mL) and GU (1.8 and/or 1.24 mmoL) was dissolved in DMF (30 mL). The reaction mixture was warmed at 100 °C for 3 days (tlc), and the solvent was removed under vacuum. The products were collected, washed several times with acetone, and dried at 50 °C for 2 days [39].

Polymer P-3A: FT-IR (film on KBr plate) (Fig. 1): *v* (cm^{-1}) 3434 (st. OH), 2923, 2858 (aliph. C-H), 1740 (st. C = O), 1639 (st, C = C), 1461 (st. C = N), 1054 (st. C-O), 617 (st. C–Cl). ^{1}H-NMR (DMSO-d_6) (Fig. 4): δ (ppm) = 1.2 (*s*, OH), 2.79–2.96 (*m*, CH_2 (protons m)), 3–3.27 (*m*, CH (protons b)), 3.81–3.9 (*m*, CH (protons c, e)), 4.09–4.18 (*m*, CH, CH_2 (protons a, l)), 4.38–4.44 (*m*, CH_2, CH (protons g, d)), 5.67–5.71 (*m*, CH (protons s, o)), 6.26 (*m*, CH (protons f)), 6.49, (*m*, CH (protons k)), 7.67 (CH (protons j)), 7.91, 10.71 (*s*, NH (protons i, q)).

Polymer P-3B: FT-IR (film on KBr plate) (Fig. 1): *v* (cm^{-1}) 3423 (st. OH), 2937 (aliph. C-H), 1697 (st. C = O), 1632 (st, C = C), 1383 (st. C = N), 1045 (st. C-O), 455 (st. C–Br). ^{1}H-NMR (DMSO-d_6) (Fig. 4): δ (ppm) = 1.16–1.24 (*m*, CH_3 (protons h)), 2.73–2.89 (*m*, CH_2 (protons m)), 3.05–3.13 (*m*, CH (protons b)), 3.53–3.91 (*m*, CH (protons c, e)), 4.03–4.42 (*m*, CH, CH_2 (protons a, g, l, o, s, f)), 5.09 (*m*, CH (protons d)), 5.68–5.70, (*m*, CH (protons k)), 6.47 (CH (protons j)), 7.92, 10.63 (*s*, NH (protons i, q)), 7.13 (*s* OH (protons p)).

Synthesis of polyvinyl alcohol-EPCH-grafted-GU (P-4)

Polyvinyl alcohol (0.5 g) was dissolved in DMF (30 mL), and GU (0.5 g), EPCH (0.6 mL), and sodium hydroxide (0.3 g) were added, respectively. The reaction mixture was warmed at 100 °C for 24 h. The solvent was removed under vacuum. The product was collected, washed several times with petroleum ether, and dried at 50 °C for 4 days [6, 39].

Polymer P-4: FT-IR (film on KBr plate) (Fig. 1): *v* (cm^{-1}) 3490 (st. OH), 3291 (st, NH), 2940 (aliph. C-H), 1664 (st. C = O), 1596 (st, C = C), 1473 (st. C = N), 1224 (st. C–C), 1101 (st. C-O). ^{1}H-NMR (DMSO-d_6) (Fig. 5): δ (ppm) = 1.35–1.44 (*m*, CH_2 (protons a)), 1.78 (*s*, OH (protons l)), 2.49–2.51 (*m*, CH (protons b)), 2.73–2.89 (*m*, CH_2 (protons c, f)), 3.13–3.31 (*m*, CH (protons d)), 3.85–4.43 (*m*, CH, CH_2

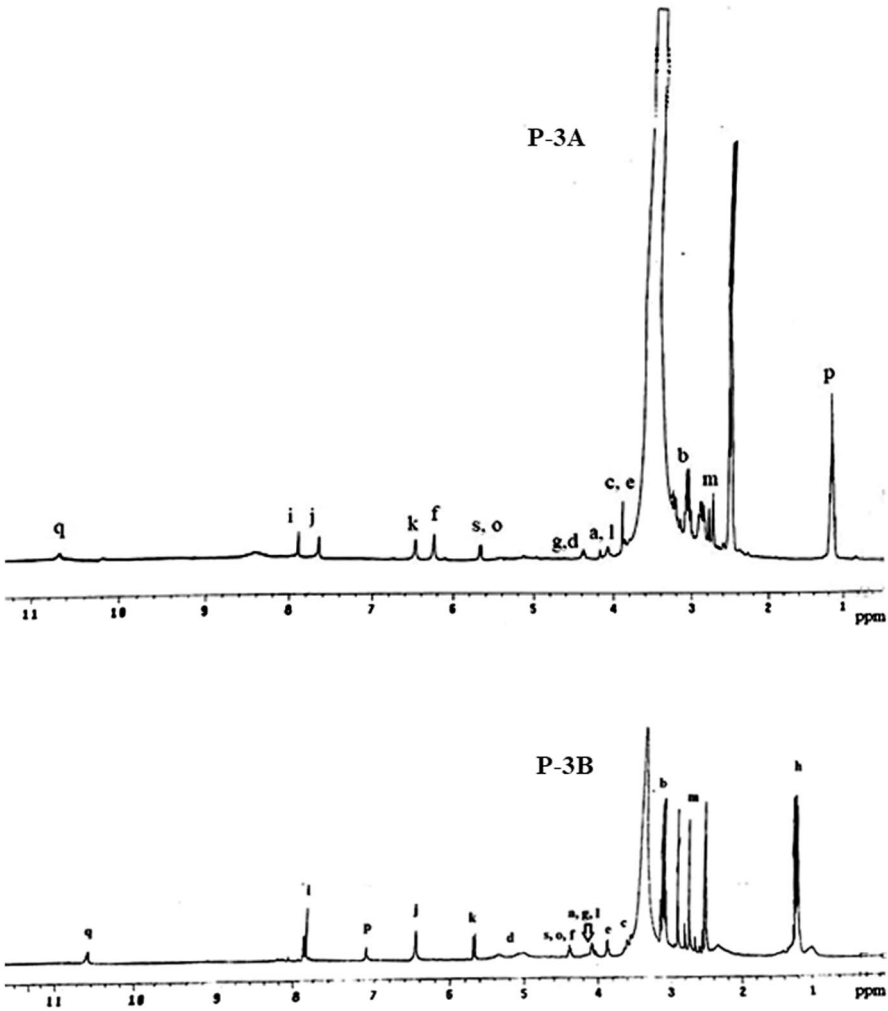

Fig. 4 ^{1}H-NMR spectra of polymers P-3A and P-3B

(protons k, m, p, q)), 5.64–5.74 (*m*, CH (protons j)), 6.92–7.01 (ar. CH (protons i)), 7.86 (*s*, OH (protons e)), 7.94, 8.46 (*s*, NH (protons h, g)).

Synthesis of chitosan-EPCH-grafted-GU (P-5)

Carbohydrate CS (0.4 g) was dissolved in 10% acetic acid solution to which GU (0.4 g), EPCH (0.4 mL), and sodium hydroxide (0.35 g) were added, respectively. The reaction mixture was warmed at 100 °C for 24 h. The solvent was removed by under vacuum. The resulted polymers were collected, washed several times with acetone/water (5:1), and dried at 50 °C for 4 days [6, 39].

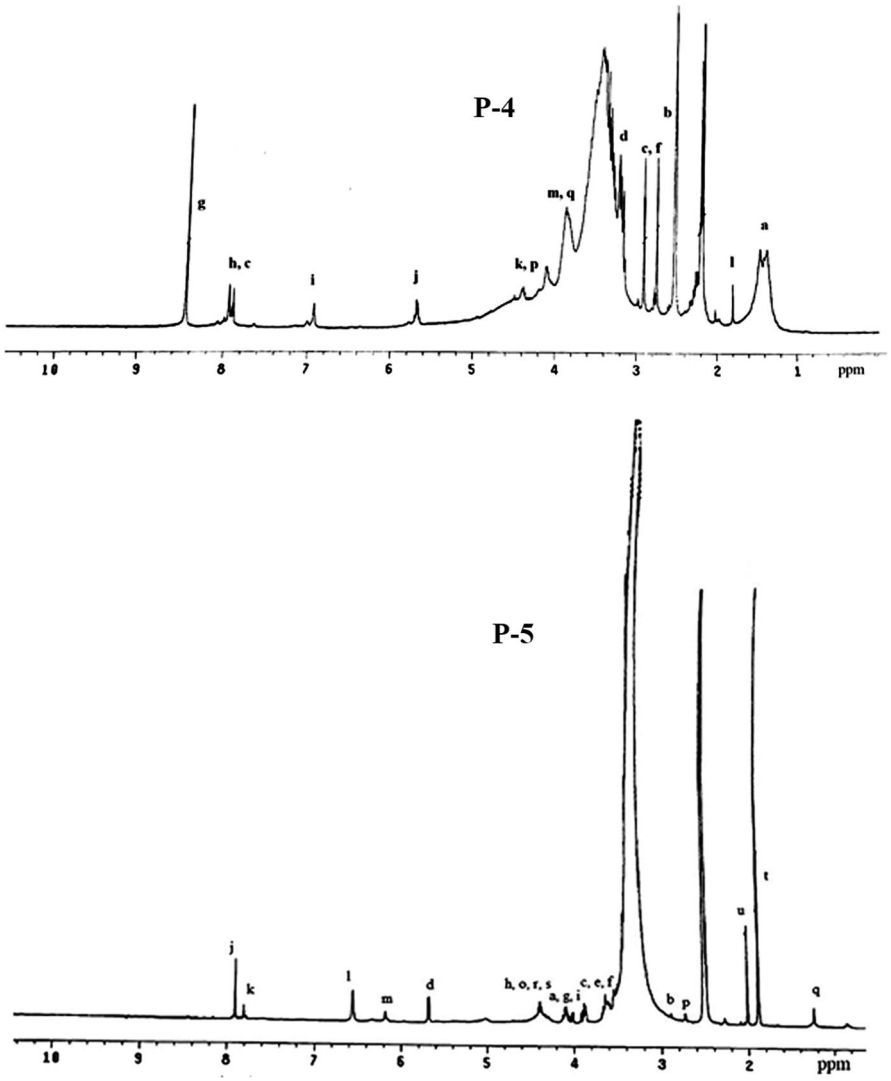

Fig. 5 ^{1}H-NMR spectra of polymers P-4 and P-5

Polymer P-5: FT-IR (film on KBr plate) (Fig. 1): *v* (cm^{-1}) 3465 (st. OH), 3370 (st, NH), 2943 (aliph. C-H), 1661 (st. C = O), 1554 (st, C = C), 1415 (st. C = N), 1265 (st. C–C), 1115 (st. C-O). ^{1}H-NMR (DMSO-d_6) (Fig. 5): δ (ppm) = 1.23, 1.88, 2 (*s*, OH (protons q, t, u)), 2.72 (*d*, CH_2 (protons p), 2.91 (*m*, CH (protons b)), 3.43–3.65 (*m*, CH (protons c, e)), 3.83–4.17 (*m*, CH_2 (protons a, g, i, d)), 4.31–4.41 (*m,* CH (protons h, o, r, s)), 5.68–5.7 (*m*, CH (protons f)), 6.18 (*d*, CH (protons m)), 6.56 (*s*, ar. CH (protons l)), 7.81, 7.91 (*s*, NH (protons k, j)).

Characterization

FT-IR spectra were recorded on Bruker, Tensor 27FT-IR spectrophotometer with frequency range 4000 cm^{-1} to 400 cm^{-1} with KBr pellets (Central Lab. Tanta University, Egypt).

^{1}H-NMR spectra were measured in DMSO-$d_6$on a Varian Mercury VX-300 (300 MHz) NMR spectrometer (Nuclear Magnetic Resonance Lab, Faculty of Science, Cairo University, Giza, Egypt) and (Nuclear Magnetic Resonance Lab, Kafrelsheikh University, Egypt).

TGA data were obtained by using Shimadzu Thermal Analyzer system at a heating rate of 10 °C/min, sample weight of 5–6 mg under nitrogen (20 mL/min) flow. The range investigated ranged from 30–400 °C (Central Lab. Tanta University, Egypt).

The number-average molecular weights (M_n), weight-average molecular weights (M_w), and polydispersity (M_w/M_n) were determined by using gel permeation chromatography (GPC) analysis with refractive index (RI) detector. RI measurements were carried out using an instrument composed of a Waters 1515 isocratic pump, a 2414 differential refractive index detector, and a column-heating module with Shodex KF-804, KF-803, and KF-802.5 columns in series. The columns were eluted with DMF (preservative-free HPLC grade, Fisher Chemical Company) at 40 °C at 1.0 mL min^{-1} and were calibrated using 14 monodisperse polystyrene standards (Alfa Aesar).

Biological activities of polymer conjugates of PVA, CS and CL with GU

Antifungal activity of polymer conjugates with GU

Antifungal activity was tested against two pathogenic strains: the mold, *Aspergillus fumigatus* (RCMB 002008), and the yeast *Candida albicans* (R9CMB 005003). The pathogenic strains were obtained from the regional center of mycology, and biotechnology (RCMB), Al-Azhar University, Egypt. Ketoconazole was purchased from commercial markets. GU and the nine synthetic polymer conjugates, P-1A, P-1B, P-2A, P-2B, P-3A, P-3B, P-4 and P-5, were dissolved and/or suspended in distilled water in a final concentration of 50 mg/mL. Ketoconazole was used as a positive control or reference drug at a concentration of 100 µg/mL. The fungal strains were cultured on Sabouraud dextrose agar media and incubated for 24 h at 35 °C. Colonies of *Candida albicans* and *Aspergillus fumigatus* were transferred into 0.9% physiological saline or distilled water amended with 0.1% Tween 20 to resuspend the colonies, respectively. 3×10^6 conidia/mL was counted using hemocytometer and then diluted into 3×10^5 conidia/mL. The previous suspension was poured on the media supplemented with 2% glucose. Sterilized disks (6 mm) were soaked separately with 100 µL of each polymer conjugate and the reference drug and then placed over the plate. Ketoconazole, a standard antifungal drug, was used as a positive control, and sterile distilled water was used as a negative control, and

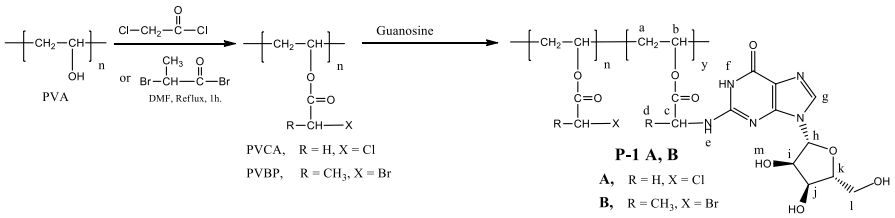

Scheme 1 Synthesis of PVCA, PVBP, and their grafting with GU

the samples were incubated at 35 °C for 48 h. The inhibition zone was measured in millimeters (mm) [42].

In vivo anticancer activity of polymer conjugates of PVA, CS and CL with GU

GU and eight polymer conjugates have been evaluated as anticancer agents. Sixty-six female albino CD1 mice (20 ± 2 g) were purchased from National Research Center, Cairo, Egypt. Mice were transferred into an animal facility in the Zoology Department, Faculty of Science, Tanta University. Mice left for acclimatization for one week before starting the experiment. Mice were then divided randomly into eleven groups ($n = 6$). All groups were inoculated with 1×10^6 EAC cells/mouse intraperitoneal (i.p.). After 24 h, Gp1 was served as EAC-bearing mice alone, and Gp2 was injected with CIS (2 mg/Kg/6 days). From Gp3–11 were injected with GU and polymer conjugates; P-1A, P-1B, P-2A, P-2B, P-3A, P-3B, P-4, and P-5, daily for six days, respectively. On day 14, all groups were sacrificed to assess the tumor volumes, total tumor cell counts and to determine the live and dead tumor cell counts [43–45].

Statistical analysis

One-way analysis of variance (ANOVA) was used to assess significant differences among treated groups. Dunnet test was used to compare all groups against the control group to show the significant effect of treatment. The data are presented as mean ± SD.

Results and discussion

FT-IR of macromolecular polymer conjugates of PVA, CS and CL with GU

In this study, PVA, CS and CL were treated with chloroacetyl chloride and 2-bromopropionyl bromide to afford the macromolecular halo polymers as shown in Schemes 1, 2 amd 3. FT-IR spectra of PVCA and PVBP illustrated the stretching carbonyl groups (C = O) at 1736, 1723 cm^{-1}, C–Cl at 641 cm^{-1} and C–Br at 507 cm^{-1}, respectively. Also, CSCA and CSBP displayed the carbonyl groups (C = O) at 1737 and 1705, C–Cl at 781 and C–Br at 634 cm^{-1}, respectively. Moreover, CLCA and

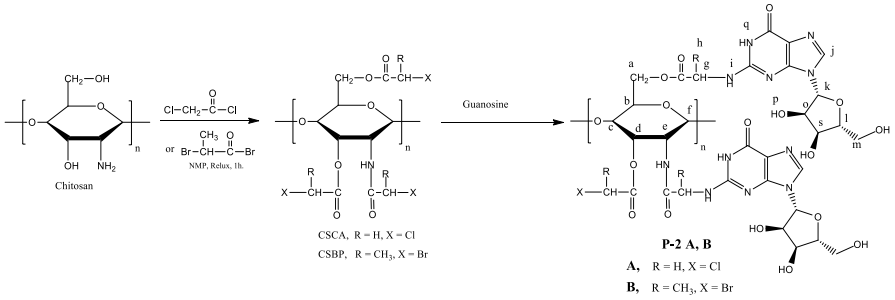

Scheme 2 Synthesis of CSCA, CSBP, and their grafting with GU

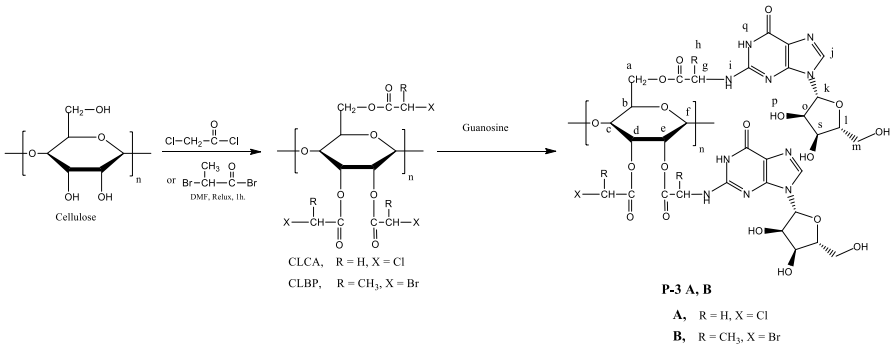

Scheme 3 Synthesis of CLCA, CLBP, and their grafting with GU

CLBP showed the stretching carbonyl groups (C = O) at 1740, 1741 cm^{-1}, C–Cl at 797 cm^{-1} and C–Br at 624 cm^{-1}, respectively. The appearance of these new peaks is due to the bounding of chloroacetyl chloride and 2-bromopropionyl bromide on the polymer chains [28, 41]. GU is chemically linked to the halo polymers using TEA as a catalyst to afford polymer conjugates P-1A, P-1B, P-2A, P-2B, P-3A, and P-3B, as mentioned in Schemes 1, 2 amd 3 [31]. FT-IR spectra of P-1A and P-1B showed the stretching hydroxyl (O–H), amino (N–H) groups in the range 3458–3330 cm^{-1}, and the stretching carbonyl peaks (C = O) at 1690 and (1697, 1683) cm^{-1}, respectively. Similarly, FT-IR spectra of P-2A and P-2B displayed the stretching O–H and N–H groups of GU in the range 3467–3066 cm^{-1} and the carbonyl peaks (C = O) at 1692 and 1695 cm^{-1}, respectively. In addition, polymers P-3A and P-3B illustrated the stretching O–H and N–H groups in the range 3434–3423 cm^{-1} and the carbonyl peaks (C = O) at 1740 and 1697 cm^{-1}, respectively. Moreover, the amino group of GU was bonded to the hydroxyl groups and/or amino groups of PVA or CS by using EPCH as a linker to afford polymers, P-4 and P-5, respectively, as shown in Scheme 4. Sodium hydroxide was used to facilitate the connection of the terminal-halo moiety of EPCH with the amino groups of GU. In addition, it is used for opening of oxirane ring to link through the hydroxyl groups of PVA, amino, and hydroxyl groups of CS. Their FT-IR spectra provided stretching O–H and N–H groups at the range 3490–3291 and the carbonyl groups of GU moieties at 1664 and 1661 cm^{-1},

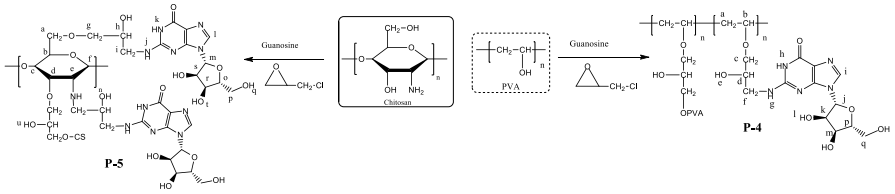

Scheme 4 Grafting of PVA and CS with GU via EPCH

respectively. The new characteristic peaks of GU moiety are compatible with previous studies [46, 47].

^{1}H-NMR, GPC and degree of grafting of polymer conjugates of PVA, CS and CL with GU

^{1}H-NMR spectra of the resulted macromolecular polymer conjugates are shown in Figs. 5, 6 and 7. ^{1}H-NMR spectra of polymer conjugates P-1A and P-1B showed multiplet -CH_2 and -CH protons of modified PVA and GU in the range 1.22–4.79 ppm and aromatic –CH protons of GU moieties at 6.35 and 6.32 ppm, respectively. Their singlet –NH protons displayed at close values of (7.67, 8.16) and (7.77, 8.15), respectively. The multiplet methyl (-CH_3) protons of polymer P-1B appeared at 1.42–1.74 ppm. Polymer P-2A showed the hydroxyl protons of GU moiety at 1.86 ppm, -CH, -CH_2 protons of CS and GU moieties in the range 2.76–6.71 ppm and NH protons at 8.19, 8.84 ppm. Polymer P-2B illustrated methyl protons at 1.96 ppm, – CH, –CH_2 protons of CS and GU moieties in the range 2.76–6.69 ppm, the hydroxyl protons of GU moiety at 8.56 ppm and NH protons at 8.65, 8.78 ppm. Polymers, P-3A and P-3B displayed multiplet –CH_2 and –CH protons of CL, chloroacetyl chloride, 2-bromopropionyl bromide and GU in the ranges (2.79–7.67) and (2.73–6.47) ppm, respectively. Also, they showed singlet

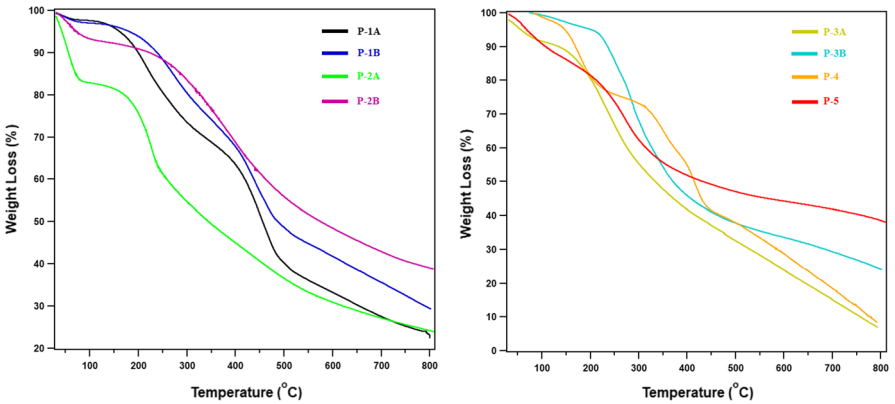

Fig. 6 TGA of polymer conjugates; P-1A, P-1B, P-2A, P-2B, P-3A, P-3B, P-4, and P-5

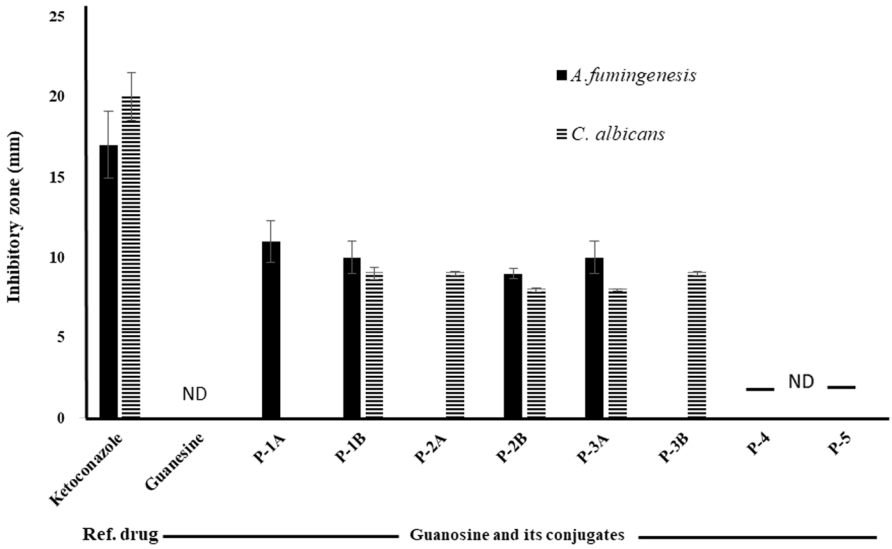

Fig. 7 Antifungal activity of GU and polymer conjugates P-1A, P-1B, P-2A, P-2B, P-3A, P-3B, P-4, and P-5 against *Aspergillus fumigatus and Candida albicans*

–NH protons at (7.91, 10.71) and (7.92, 10.63), respectively. Polymer P-3B provided the multiplet methyl (-CH_3) protons at 1.16–1.24 ppm. Polymer P-4 provided singlet –OH protons at 1.78, 7.86 ppm and multiplet -CH_2, -CH protons of PVA, the opened EPCH linker and GU in the range 1.35–4.43 ppm. Moreover, multiplet aromatic –CH protons were displayed at 6.92–7.01 ppm and the singlet –NH protons at 7.94 and 8.46 ppm. In addition, polymer P-5 provided the singlet hydroxyl protons at 1.23, 1.88, 2 ppm, –CH, –CH_2 protons of CS and GU moieties in the range 2.72–6.56 ppm and NH protons at 7.81, 7.91 ppm. The proton peaks of grafted GU moieties along the polymer chains are agreed with previous studies [48, 49]. The number average molecular weight (M_n), weight average molecular weight (M_w) and polydispersity of polymer conjugates P-1A, P-1B, P-3A and P-3B are shown in Table 1. Their polydispersities are in the range 1.002–1.715, indicating that the polymer chains have close molecular weights. The degrees of grafting of the prepared polymer conjugates are shown in Table 2 as previously described [50, 51]. Grafted polymer conjugates revealed a reasonable grafting degree ranging within 35–66%.

Table 1 GPC of polymers P-1A, P-1B, P-3A, and P-3B

Polymer conjugate	M_n (Daltons)	M_w (Daltons)	M_w/M_n
P-1A	14,954	25,651	1.715
P-1B	47,785	66,995	1.402
P-3A	12,637	20,098	1.590
P-3B	362,294	363,022	1.002

Table 2 Calculated degree of grafting (%) of polymer conjugates

Polymer conjugate	Degree of grafting (%)
PVCA	93
PVBP	95
CSCA	86
CSBP	90
CLCA	84
CLBP	86
P-1A	57
P-1B	46
P-2A	52
P-2B	39
P-3A	55
P-3B	35
P-4	63
P-5	66

Among polymer conjugates, polymers P-4 and P-5 showed the highest degree of grafting. Thus, the grafting of GU on PVA and CS by using EPCH is a better way of grafting than using chloroacetyl chloride or 2-bromopropionyl bromide.

Thermogravimetric analysis (TGA) of new conjugates of PVA, CS and CL with GU

The thermogravimetric analysis curves of modified PVA, CS and CL grafted with GU are shown in Fig. 6. CS and modified CS with chloroacetyl chloride illustrated two degradation steps of weight loss [40], and CL grafted with chloroacetyl chloride provided two stages of decomposition [28]. TGA showed that conjugates: P-1A, P-1B, P-2A, P-2B, P-3A, P-3B, P-4, and P-5 undergo two-step degradation of weight loss. The first degradation steps (below 150 °C) observed in all polymer conjugates are due to the loss of absorbed and bound water. The second stages of degradation for all polymers are mainly referred to random decomposition of the aliphatic polymer chains and the grafted GU at raised temperatures (up to 800 °C). The residual weights for all polymers ranged from 8 to 40% at 800 °C indicating their high thermal stability. Polymer P-1B exhibited lower degradation rates and residual weight than that of polymer P-1A at the same temperatures resulting in its higher thermal stability than P-1A. Similarly, polymer P-2B provided higher thermal stability than polymer P-2A. Furthermore, polymer P-3B provided better thermal stability than polymer P-3A. So, we can conclude that the functionalized PVA, CS and CL with GU via 2-bromopropionyl bromide are thermally stable than their analogs with chloroacetyl chloride. TGA illustrated that polymer P-4 displayed lower degradation rates and residual weight than that of polymers, P-1A and P-1B and so lower thermal stability, which may be due to the difference in method of chemical grafting. In

addition, polymer P-5 showed higher thermal stability than P-2A and lower thermal stability than P-2B with a high residual weight of 38.58% at 800 °C.

Antifungal activity of new conjugates of PVA, CS and CL with GU

The antifungal activity of GU and its polymer conjugates were tested against two pathogenic fungal strains, *Aspergillus fumigatus* and *Candida albicans* (Fig. 7). In the present study, GU, P-4 and P-5 did not revealed antifungal activity against the two fungal strains. The antifungal sensitivity of polymer conjugates against pathogenic strains was tested by measuring the diameter of their inhibitory zones. *C. albicans* was sensitive to five polymer conjugates, P-1B, P-2A, P-2B, P-3A, and P-3B, with inhibitory zones of 9 ± 0.4, 9 ± 0.11, 8 ± 0.1, 8 ± 0.06 and 9 ± 0.11 mm, respectively. Moreover, polymer conjugates, P-1A, P-1B, P-2B, and P-3A, revealed antifungal activity on *A. fumigatus* with inhibitory zones of 11 ± 1.3, 10 ± 1, 9 ± 0.33 and 10 ± 1 mm, respectively. The study of Avila et al. was in accordance with our data and revealed that two GU analogs have anti-protozoal activity against *Trypanosoma cruzi*, *T. rangeli* and *Leishmania spp* in vitro. Nucleoside analogs have antimicrobial activities by different pathways on eukaryotic cells [52]. Analogs of nucleoside could enter the microbes membrane via membrane transporters and then cycled through the nucleoside salvage pathway where they were activated by deoxyribonucleoside kinases [53]. Interestingly, the antifungal behavior of the new conjugate may be due to the new chemical combination of GU with the modified PVA, CS, CL, the structure–activity relationship, and the presence of some functional groups as N–H, Cl, Br or OH along the chains of polymer conjugates. Thus, chemical grafting of PVA, CS and Cl with GU resulted in improving their antifungal activity.

In vivo antitumor activity of new conjugates of PVA, CS and CL with GU

As compared to group of EAC-bearing mice alone, the results showed that all EAC-bearing mice groups injected with synthetic polymer conjugates, P-1A, P-1B, P-2A, P-2B, P-3B, P-4 and P-5 except P-3A group showed significant reduction in total tumor volume (Fig. 8). Conjugates P-1A and P-4 provided small tumor volume values close to CIS. % B.Wt changes of the previous groups were decreased as compared to % B.Wt changes in EAC-bearing mice alone. In addition, the total tumor and the total live tumor counts were significantly decreased in all groups under investigation except P-3A group (Table 3). Among all polymer conjugates, P-1A, P-3B, P-4, and P-5 showed high decrease in total tumor volume and % B.Wt changes as compared to CIS and GU groups. Thus, the chemical grafting of GU on PVA, CS and CL via chloroacetyl chloride, 2-bromopropionyl bromide and EPCH is a promising strategy for enhancing the antitumor activity of GU. As a relation between the degree of grafting (Table 2) and antitumor activity, polymer conjugates, P-1A, P-4 and P-5, showed high degree of grafting and consequently high antitumor activity against EAC-bearing mice. In recent studies, supramolecular hydrogel, isoguanosine-borate-guanosine displayed highly antitumor effect through inducing tumor cell apoptosis, excellent inhibition effect of tumor repetition and serve as a

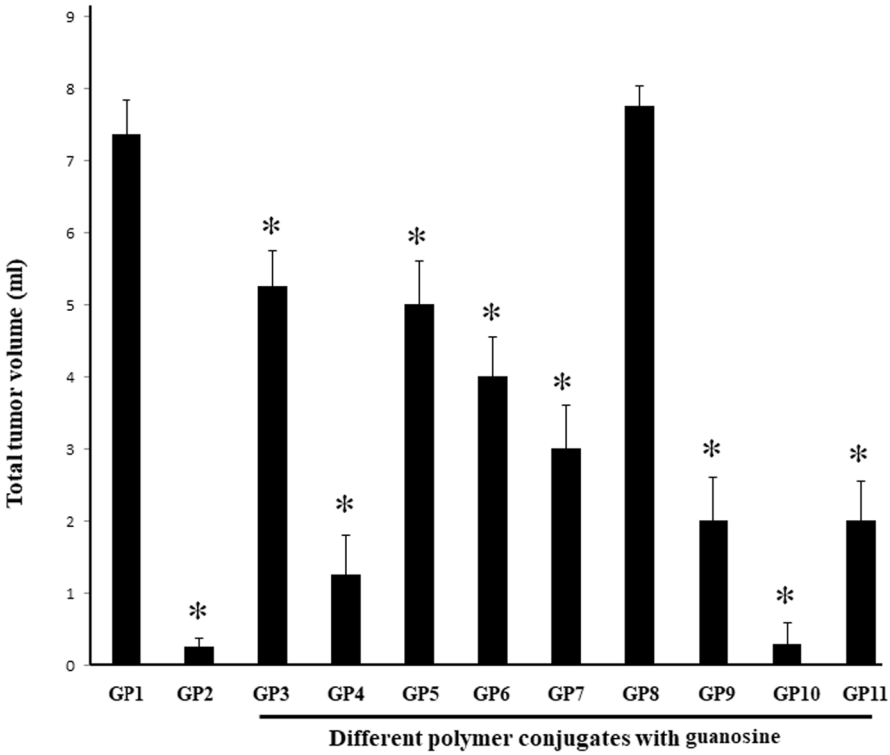

Fig. 8 Total tumor volume of different groups of positive control, CIS, GU and its polymer conjugates. **Gp1**: EAC-bearing mice, **Gp2**: EAC/CIS (2 mg/kg), **Gp3**: EAC/GU (10 mg), **Gp4**: EAC/P-1A (10 mg), **Gp5**: EAC/P-1B (10 mg), **Gp6**: EAC/P-2A (10 mg), **Gp7**: EAC/P-2B (10 mg), **Gp8**: EAC/P-3A (10 mg), **Gp9**: EAC/P-3B (10 mg), **Gp10**: EAC/P-4 (10 mg), **Gp11**: EAC/P-5 (10 mg)

Table 3 Body weight changes (% B.Wt), total EAC count and viability of the different groups under study

Group	% B.Wt Change	T.C.C ($\times 10^6$/mouse)	T.L.C ($\times 10^6$/mouse)	T.D.C ($\times 10^6$/mouse)
EAC-bearing mice	49.40	655 ± 42	650 ± 41	5 ± 1
EAC/CIS	− 5.95*	17 ± 4.5*	7 ± 2*	10 ± 1.5*
EAC/GU	36.46*	483 ± 19*	462 ± 12*	21 ± 2*
EAC/P-1A	10.55*	142 ± 5*	131 ± 6*	11 ± 1.3*
EAC/P-1B	33.54*	390 ± 19*	378 ± 16*	12 ± 1.5*
EAC/P-2A	29.32*	385 ± 17*	375 ± 15*	10 ± 1.6*
EAC/P-2B	23.07*	310 ± 14*	301 ± 12*	9 ± 1.3*
EAC/P-3A	39.10	520 ± 26	501 ± 23*	19 ± 2.1*
EAC/P-3B	14.88*	205 ± 8*	195 ± 6*	10 ± 1.1*
EAC/P-4	− 2.76*	27 ± 6*	19 ± 4*	8 ± 1.3*
EAC/P-5	15.35*	210 ± 9*	202 ± 7*	8 ± 1.3*

CIS (2 mg/kg/6 days), GU and all polymer conjugates were injected as 10 mg/Kg/6 days

dual-function hydrogel system as drug carrier and anticancer [38, 54]. GU exhibited effective treatment against P388 leukemia by the combination of various fluorinated pyrimidines, 5-fluorouracil, 5-fluorouridine and 5-fluoro-2′-deoxyuridine [55].

Conclusion

In the present study, conjugation of PVA, CS and CL with GU has been successfully developed and characterized by using FTIR, ^{1}H-NMR, GPC and TGA techniques. GU showed no antifungal activity, while most of the prepared macromolecular polymer conjugates showed significant antifungal activity against *Aspergillus fumigatus* and *Candida albicans*. In addition, seven of the synthesized eight polymer conjugates illustrated enhanced antitumor effect against EAC-bearing mice as compared to GU. Especially, poly(vinyl chloroacetate)-grafted-GU (P-1A), cellulose bromopropionate-grafted-GU (P-3B), polyvinyl alcohol-EPCH-grafted-GU (P-4), and chitosan-EPCH-grafted-GU (P-5) showed potent antitumor activity against EAC-bearing mice. Thus, chemical grafting of GU on PVA, CS and CL is a candidate way for improving its biomedical applications.

Funding Open access funding provided by The Science, Technology & Innovation Funding Authority (STDF) in cooperation with The Egyptian Knowledge Bank (EKB). This study was funded by the authors, and no other funding was received.

Declarations

Conflict of interest The authors declared that there is no conflict of interest.

Open Access This article is licensed under a Creative Commons Attribution 4.0 International License, which permits use, sharing, adaptation, distribution and reproduction in any medium or format, as long as you give appropriate credit to the original author(s) and the source, provide a link to the Creative Commons licence, and indicate if changes were made. The images or other third party material in this article are included in the article's Creative Commons licence, unless indicated otherwise in a credit line to the material. If material is not included in the article's Creative Commons licence and your intended use is not permitted by statutory regulation or exceeds the permitted use, you will need to obtain permission directly from the copyright holder. To view a copy of this licence, visit http://creativecommons.org/licenses/by/4.0/.

References

1. Ruiz S, Tamayo JA, Delgado OJ, Navia Porras DP, Valencia Zapata ME, Mina Hernandez JH, Valencia CH, Zuluaga F, Grande Tovar CD (2019) Antimicrobial films based on nanocomposites of chitosan/poly (vinyl alcohol)/graphene oxide for biomedical applications. Biomolecules 9:109
2. Jantas R, Draczyński Z, Herczyńska L, Stawski D (2012) Poly (vinyl alcohol)-salicylic acid conjugate: synthesis and characterization. Am J Polym Sci 2:79–84
3. Marin E, Rojas J, Ciro Y (2014) A review of polyvinyl alcohol derivatives: Promising materials for pharmaceutical and biomedical applications. Afr J Pharm Pharmacol 8:674–684
4. Liu YL, Chiu YC (2003) Novel approach to the chemical modification of poly (vinyl alcohol): phosphorylation. J Polym Sci Part A: Polym Chem 41:1107–1113

5. Buhus G, Popa M, Peptu C, Desbrieres J (2007) Hydrogels based on carboxymethylcellulose and poly (vinyl alcohol) for controlled loading and release of chloramphenicol. CERMAV. J Optoelectron Adv Mater 9:3445
6. Garnica-Palafox I, Sánchez-Arévalo F, Velasquillo C, García-Carvajal Z, García-López J, Ortega-Sánchez C, Ibarra C, Luna-Bárcenas G, Solís-Arrieta L (2014) Mechanical and structural response of a hybrid hydrogel based on chitosan and poly (vinyl alcohol) cross-linked with epichlorohydrin for potential use in tissue engineering. J Biomater Sci Polym Ed 25:32–50
7. Yang J, Yu H, Wang L, Liu J, Liu X, Hong Y, Huang Y, Ren S (2022) Advances in adhesive hydrogels for tissue engineering. Eur Polym J 172:111241
8. Altun T (2019) Chitosan-coated sour cherry kernel shell beads: an adsorbent for removal of Cr (VI) from acidic solutions. J Anal Sci Technol 10:14
9. Gao Y, Yuling W (2022) Recent advances of chitosan-based nanoparticles for biomedical and biotechnological applications. Int J Appl Polym Sci 203:379–388
10. Niaz T, Shabbir S, Manzoor S, Rehman A, Rahman A, Nasir H, Imran M (2016) Antihypertensive nano-ceuticales based on chitosan biopolymer: Physico-chemical evaluation and release kinetics. Carbohydr Polym 142:268–274
11. Hosseini SM, Mazinani S, Abdouss M, Kalhor H, Kalantari K, Amiri IS, Ramezani Z (2022) Designing chitosan nanoparticles embedded into graphene oxide as a drug delivery system. Polym Bull 79:541–554
12. Batista P, Castro P, Madureira AR, Sarmento B, Pintado M (2019) Development and characterization of chitosan microparticles-in-films for buccal delivery of bioactive peptides. Pharmaceuticals 12:32
13. Yadav M, Goswami P, Paritosh K, Kumar M, Pareek N, Vivekanand V (2019) Seafood waste: a source for preparation of commercially employable chitin/chitosan materials. Bioresour Bioprocess 6:8
14. Chadha U, Bhardwaj P, Selvaraj SK, Kumari K, Isaac TS, Panjwani M, Kulkarni K, Mathew RM, Satheesh AM, Pal A (2022) Advances in chitosan biopolymer composite materials: from bioengineering, wastewater treatment to agricultural applications. Polymers 14:958
15. Refaee AA, El-Naggar ME, Mostafa TB, Elshaarawy RF, Nasr A (2022) Nano-bio finishing of cotton fabric with quaternized chitosan Schiff base-TiO2-ZnO nanocomposites for antimicrobial and UV protection applications. Eur Polym J 166:111040
16. Sahin M, Kocak N, Arslan G, Ucan HI (2011) Synthesis of crosslinked chitosan with epichlorohydrin possessing two novel polymeric ligands and its use in metal removal. J Inorg Organomet Polym Mater 21:69–80
17. Gutha Y, Zhang Y, Zhang W, Jiao X (2017) Magnetic-epichlorohydrin crosslinked chitosan schiff's base (m-ECCSB) as a novel adsorbent for the removal of Cu (II) ions from aqueous environment. Int J Biol Macromol 97:85–98
18. Hastuti B, Masykur A, Hadi S (2016) Modification of chitosan by swelling and crosslinking using epichlorohydrin as heavy metal Cr (VI) adsorbent in batik industry wastes. IOP Conf Ser: Mater Sci Eng 5:12020
19. Li CG, Wang F, Peng WG, He YH (2013) Preparation of chitosan and epichlorohydrin crosslinked adsorbents and adsorption property of dyes. Appl Mech Mater 65:84–587
20. Austero MS, Donius AE, Wegst UG, Schauer CL (2012) New crosslinkers for electrospun chitosan fibre mats. Anal Chem 9:2551–2562
21. Zhong Z, Xing R, Liu S, Wang L, Cai S, Li P (2008) Synthesis of acyl thiourea derivatives of chitosan and their antimicrobial activities in vitro. Carbohydr Res 343:566–570
22. Jenkins DW, Hudson SM (2001) Review of vinyl graft copolymerization featuring recent advances toward controlled radical-based reactions and illustrated with chitin/chitosan trunk polymers. Chem Rev 101:3245–3274
23. Abdel-Nasser E, Hafez JA, Badawy RM, Mohamed HI, Rizk SA (2019) Design, synthesis of spiro quinazolinone compacted with chitosan through DFT approach for interference the antimicrobial activity. Open Chem J 3:33–42
24. Elbarbary AA, Kenawy E-R, Hamada EG, Edries TB, Meshrif WS (2021) Insecticidal activity of some synthesized 1, 3, 4-oxadiazole derivatives grafted on chitosan and polymethylmethacrylate against the cotton leafworm Spodoptera littoralis. Int J Biol Macromol 180:539–546
25. Peng B, Yao Z, Wang X, Crombeen M, Sweeney DG, Tam KC (2020) Cellulose-based materials in wastewater treatment of petroleum industry. Green Energy Environ 5:37–49

26. Bidhendi AJ, Chebli Y, Geitmann A (2020) Fluorescence visualization of cellulose and pectin in the primary plant cell wall. J Microsc 278:164–181
27. Dehabadi L, Wilson LD (2014) Polysaccharide-based materials and their adsorption properties in aqueous solution. Carbohydr polym 113:471–479
28. Coskun M, Temüz MM (2005) Grafting studies onto cellulose by atom-transfer radical polymerization. Polym Int 54:342–347
29. Çankaya N, Temüz MM, Yakuphanoglu F (2018) Grafting of some monomers onto cellulose by atom transfer radical polymerization. Electrical conductivity and thermal properties of resulting copolymers. Cellul Chem Technol 52:19–26
30. Krouit M, Granet R, Krausz P (2008) Photobactericidal plastic films based on cellulose esterified by chloroacetate and a cationic porphyrin. Bioorg Med Chem 16:10091–10097
31. Tan W, Guo Z, Chen Q, Dong F, Li Q (2017) Synthesis of aminopyridinium-grafted starch derivatives and evaluation of their antioxidant property. Starch 69:1600259
32. Osanlou F, Nemati F, Sabaqian S (2017) An eco-friendly and magnetized biopolymer cellulose-based heterogeneous acid catalyst for facile synthesis of functionalized pyrimido [4, 5-b] quinolines and indeno fused pyrido [2, 3-d] pyrimidines in water. Res Chem Intermed 43:2159–2174
33. Bettio LE, Gil-Mohapel J, Rodrigues AL (2016) Guanosine and its role in neuropathologies. Purinergic Signal 12:411–426
34. Dačević M, Isaković A, Podolski-Renić A, Isaković AM, Stanković T, Milošević Z, Rakić L, Ruždijić S, Pešić M (2013) Purine nucleoside analog-sulfinosine modulates diverse mechanisms of cancer progression in multi-drug resistant cancer cell lines. PloS One 8:e54044
35. Naliwaiko K, Luvizon AC, Donatti L, Chammas R, Mercadante AF, Zanata SM, Nakao L (2008) Guanosine promotes B16F10 melanoma cell differentiation through PKC–ERK 1/2 pathway. Chem Biol Interact 173:122–128
36. Oliveira KA, Dal-Cim TA, Lopes FG, Nedel CB, Tasca C (2017) Guanosine promotes cytotoxicity via adenosine receptors and induces apoptosis in temozolomide-treated A172 glioma cells. Purinergic Signal 13:305–318
37. Chen M, Lin W, Hong L, Ji N, Zhao H (2019) The development and lifetime stability improvement of guanosine-based supramolecular hydrogels through optimized structure. Biomed Res Int 2019:87
38. Zhao H, Feng H, Liu J, Tang F, Du Y, Ji N, Xie L, Zhao X, Wang Z, Chen Q (2020) Dual-functional guanosine-based hydrogel integrating localized delivery and anticancer activities for cancer therapy. Biomaterials 230:119598
39. El-Naggar SA, El-Barbary AA, Salama WM, Elkholy HM (2022) Synthesis, characterization, and biological activities of folic acid conjugates with polyvinyl alcohol, chitosan, and cellulose. J Appl Polym Sci 139:52250
40. Kenawy E-R, El-Newehy MH, Abdel-Hay FI, El-Shanshoury AE (2014) Synthesis and biocidal activity of modified poly (vinyl alcohol). Arab J Chem 7:355–361
41. Tan W, Li Q, Dong F, Chen Q, Guo Z (2017) Preparation and characterization of novel cationic chitosan derivatives bearing quaternary ammonium and phosphonium salts and assessment of their antifungal properties. Molecules 22:1438
42. Esmadi F (2013) Synthesis and characterization of some transition metal complexes of thiocarbohydrazone Schiff bases, Jordan. J Chem 8:31–43
43. El-Naggar S, El-Barbary A, Mansour M, Abdel-Shafy F, Talat S (2011) Anti-tumor activity of some 1, 3, 4-thiadiazoles and 1, 2, 4-triazine derivatives against ehrlichs ascites carcinoma. Int J Cancer Res 7:278–288
44. El-Naggar S (2011) Lack of the beneficial effects of mirazid (Commiphora molmol) when administered with chemotherapeutic agents on Ehrlich ascetic carcinoma bearing mice. Adv Biol Res 5:193–199
45. Abdelwahab MA, Ahmed A, El-Said KS, El Naggar SA, ElKholy HM (2019) Evaluation of antibacterial and anticancer properties of poly (3-hydroxybutyrate) functionalized with different amino compounds. Int J Biol Macromol 122:793–805
46. Al-Mahamad LLG (2019) Synthesis and surface characterization of new triplex polymer of Ag (I) and mixture nucleosides: cytidine and 8-bromoguanosine. Heliyon 5:e01609
47. Masuda M, Suzuki T, Friesen MD, Ravanat J-L, Cadet J, Pignatelli B, Nishino H, Ohshima H (2001) Chlorination of guanosine and other nucleosides by hypochlorous acid and myeloperoxidase of activated human neutrophils: catalysis by nicotine and trimethylamine. J Biol Chem 276:40486

48. Webber AL, Masiero S, Pieraccini S, Burley JC, Tatton AS, Iuga D, Pham TN, Spada GP, Brown SP (2011) Identifying guanosine self assembly at natural isotopic abundance by high-resolution 1H and 13C solid-state NMR spectroscopy. J Am Chem Soc 133:19777–19795
49. Djuran MI, Milinković S, Bugarĉić ID (1998) 1H NMR investigation of competitive binding of sulfur-containing peptides and guanosine 5′-monophosphate to a monofunctional platinum (II) complex. J Coord Chem 44:289–297
50. Nho Y, Chen J, Jin J (1999) Chemistry, Grafting polymerization of styrene onto preirradiated polypropylene fabric. Radiat Phys Chem 54:317–322
51. Sehgal T, Rattan S (2010) Synthesis, characterization and swelling characteristics of graft copolymerized isotactic polypropylene film. Int J Polym Sci 2010:86
52. Thomson JM, Lamont I (2019) Nucleoside analogues as antibacterial agents. Front Microbiol 10:952
53. Sun R, Wang L (2013) Inhibition of Mycoplasma pneumoniae growth by FDA-approved anticancer and antiviral nucleoside and nucleobase analogs. BMC Microbiol 13:1–12
54. Bhattacharyya T, Saha P, Dash J (2018) Guanosine-derived supramolecular hydrogels: recent developments and future opportunities. ACS Omega 3:2230–2241
55. Iigo M, Hoshi A (1984) Effect of guanosine on antitumor activity of fluorinated pyrimidines against P 388 leukemia, Cancer Chemother. Pharmacol 13:86–90

Publisher's Note Springer Nature remains neutral with regard to jurisdictional claims in published maps and institutional affiliations.